Appl. Phys. B 32, 145–152 (1983)

Applied Physics B Photophysics and Laser Chemistry

Frequency Modulation (FM) Spectroscopy

Theory of Lineshapes and Signal-to-Noise Analysis

G. C. Bjorklund and M. D. Levenson
IBM Research Laboratory, San Jose, CA 95193, USA

W. Lenth
MIT Lincoln Laboratory, P.O. Box 73, Lexington, MA 02173, USA

C. Ortiz
Instituto de Optica, Serrano 121, Madrid, Spain

Received 30 June 1983/Accepted 31 July 1983

Abstract. Frequency modulation (FM) spectroscopy is a new method of optical heterodyne spectroscopy capable of sensitive and rapid measurement of the absorption or dispersion associated with narrow spectral features. The absorption or dispersion is measured by detecting the heterodyne beat signal that occurs when the FM optical spectrum of the probe wave is distorted by the spectral feature of interest. A short historical perspective and survey of the FM spectroscopy work performed to date is presented. Expressions describing the nature of the beat signal are derived. Theoretical lineshapes for a variety of experimental conditions are given. A signal-to-noise analysis is carried out to determine the ultimate sensitivity limits.

PACS: 07.65

Frequency modulation (FM) spectroscopy is a new method of optical heterodyne spectroscopy capable of sensitive and rapid detection of absorption or dispersion features [1, 2]. As shown in Fig. 1, the output of a single-axial-mode dye laser oscillating at optical frequency ω_c is passed through a phase modulator driven sinusoidally at radio frequency ω_m to produce a pure FM optical spectrum consisting of a strong carrier at frequency ω_c with two weak sidebands at frequencies $\omega_c \pm \omega_m$. The beam is next passed through the sample containing the spectral feature of interest and the impinges on a fast square law photodetector. The Fourier component of the photodetector electrical signal at frequency ω_m is detected using standard rf techniques.

A key concept is that ω_m can be large compared to the width of the spectral feature of interest, so that, as illustrated in Fig. 2, the spectral feature can be probed by a single isolated sideband and the full spectral resolution of the original laser source is maintained. Both the absorption and dispersion associated with the spectral feature can be separately measured by monitoring the phase and amplitude of the rf heterodyne beat signal that occurs at frequency ω_m when the FM optical spectrum is distorted by the effects of the spectral feature. In contrast to traditional wavelength modulation techniques, the signal occurs at rf frequencies large compared to the linewidth of the laser source. Since single-mode dye lasers have little noise at radio frequencies, these beat signals can be detected with a high degree of sensitivity. Furthermore, the entire lineshape of the spectral feature can be scanned by tuning either ω_c or ω_m.

It should be noted that the use of sidebands for spectroscopy is not new. The Pound microwave frequency stabilizer [3] worked on this principle and the NMR techniques developed by Smaller [4] and Acrivos [5] are closely related. Standard (non-

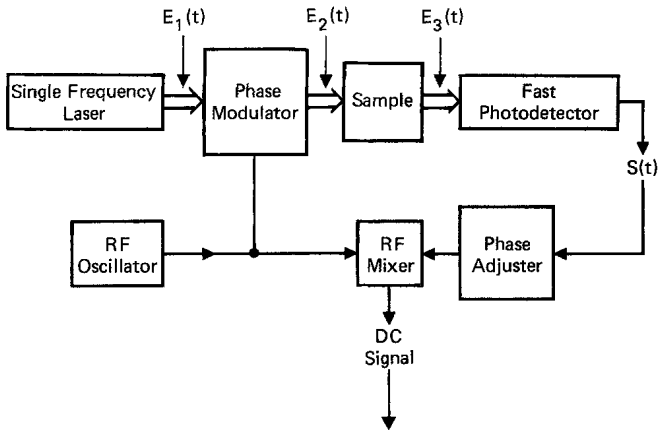

Fig. 1. A typical experimental arrangement for FM spectroscopy

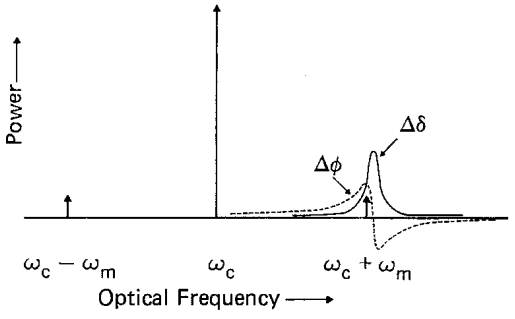

Fig. 2. Frequency domain illustration of FM spectroscopy

heterodyne) laser absorption spectroscopy with sidebands has been performed by Corcoran et al. [6], Mattick et al. [7], and Magerl et al. [8]. Heterodyne laser spectroscopy with amplitude modulated (AM) sidebands has been accomplished by Szabo [9] and Erickson [10]. Sideband techniques have recently been employed with great success to heterodyne detect signals from resonant degenerate four-wave mixing experiments [11–14]. Wavelength modulation spectroscopy with lasers, as has been done by Hinkley and Kelley [15] and Tang and Telle [16], can be viewed as heterodyne spectroscopy with very closely spaced FM sidebands. Harris et al. [17] recognized that the appearance of rf beats provides a sensitive indication of distortion of the output of an FM laser. However, the use of widely separated FM sidebands for optical heterodyne spectroscopy has only recently been accomplished and exploitation of the attendant advantages of zero-background signal, rapid response to transients, and laser limited resolution has only just begun.

Since the initial experiments with cavity resonances [1, 2], FM laser spectroscopy has been utilized to measure saturation holes in I_2 vapor [18, 19], persistent photochemical holes burned in color-center zero phonon lines [20–22], time dependent laser gain [23], two-photon absorption [24], stimulated Raman gain [25], frequency offset between a fixed frequency laser and an absorption line [26], and atomic absorption in atmospheric pressure flames [27]. Generalizations of the theory to include nonlinear effects have been performed by Hall et al. [19], Agarwal [28], Schenzle et al. [29], and Shirley [30]. Whittaker and Bjorklund [31] have extended the theory to cover arbitrarily large modulation index. Research on the use of the technique for interferometer stabilization [32] and laser frequency stabilization has continued. Several groups have reported short term laser linewidths on the order of 100 Hz [33, 34]. Recently, FM spectroscopy with widely spaced sidebands has been performed using direct injection current modulation of GaAlAs diode lasers [35]. Finally, the time resolution capability of FM spectroscopy has been demonstrated in the microsecond regime using acousto-optic chopping of a cw dye laser beam [20] and in the nanosecond regime by Gallagher et al. [36] who used a high-power pulsed dye laser of relatively standard design. The significance of the work of Gallagher et al. is that FM spectroscopy can be performed with relatively broad-band laser sources so long as the rf modulation frequency is greater than the laser bandwidth and that nonlinear optical techniques can be used to translate the high power frequency modulated laser radiation to the uv or ir spectral region. This later point has recently been demonstrated by Tran et al. [37].

Basic Principles and Theory of Lineshapes

In the limit that the modulation index $M \ll 1$, the electric field $E_2(t)$ emerging from the modulator shown in Fig. 1 is described by $E_2(t) = 1/2\tilde{E}_2(t) + \text{c.c.}$ where

$$\tilde{E}_2(t) = E_0 \left\{ -\frac{M}{2} \exp[\mathrm{i}(\omega_c - \omega_m)t] + \exp(\mathrm{i}\omega_c t) + \frac{M}{2} \exp[\mathrm{i}(\omega_c + \omega_m)t] \right\} \quad (1)$$

and E_0 is the electric field amplitude of the original laser beam. This is a pure FM optical spectrum with sidebands at frequencies $\omega_c + \omega_m$. Figure 2 shows the power spectrum and illustrates the case where the $\omega_c + \omega_m$ sideband probes a Lorentzian spectral feature.

The beam emerging from the modulator is next passed through the sample containing the spectral feature. The sample is assumed to be of length L and to have intensity absorption coefficient α and index of refraction n which are functions of the optical frequency. It is convenient to define the amplitude transmission, attenuation, and phase shift for each spectral com-

ponent $T_j=\exp(-\delta_j-i\phi_j)$, $\delta_j=\alpha_j L/2$, and $\phi_j=n_j L(\omega_c+j\omega_m)/c$, where $j=0, \pm 1$ denotes the components at ω_c, and $\omega_c\pm\omega_m$, respectively. Thus δ_j describes the amplitude attenuation and ϕ_j describes the optical phase shift experienced by each component. The transmitted field is $E_3(t)=\tilde{E}_3(t)/2+\text{c.c.}$ with

$$\tilde{E}_3(t)=E_0\left\{-T_{-1}\frac{M}{2}\exp[i(\omega_c-\omega_m)t]+T_0\exp(i\omega_c t)+T_1\frac{M}{2}\exp[i(\omega_c+\omega_m)t]\right\}. \quad (2)$$

The slowly varying intensity envelope, $I_3(t)$, of the beam impinging on the photodetector is given by $I_3(t)=c|\tilde{E}_3(t)|^2/8\pi$. Dropping terms of order M^2 and assuming that $|\delta_0-\delta_1|$, $|\delta_0-\delta_{-1}|$, $|\phi_0-\phi_1|$, and $|\phi_0-\phi_{-1}|$ are all $\ll 1$,

$$I_3(t)=\frac{cE_0^2}{8\pi}e^{-2\delta_0}[1+(\delta_{-1}-\delta_1)M\cos\omega_m t+(\phi_1+\phi_{-1}-2\phi_0)M\sin\omega_m t]. \quad (3)$$

The photodetector electrical signal is proportional to $I_3(t)$, and thus will contain a beat signal at the rf modulation frequency ω_m if $\delta_{-1}-\delta_1\neq 0$ or if $\phi_1+\phi_{-1}-2\phi_0\neq 0$. Such a signal is easily detected using standard phase sensitive rf detection techniques, as illustrated in Fig. 1. The $\cos\omega_m t$ component of the beat signal is proportional to the difference in amplitude loss experienced by the upper and lower sidebands, whereas the $\sin\omega_m t$ component is proportional to the difference between the phase shift experienced by the carrier and the average of the phase shifts experienced by the sidebands. If ω_m is small compared to the width of the spectral feature of interest, then the $\cos\omega_m t$ component is proportional to the derivative of the absorption and the $\sin\omega_m t$ component is proportional to the second derivative of the dispersion.

On the other hand, the absorption or dispersion lineshape of the spectral feature can be directly measured if ω_m is large enough that the spectral feature is probed by a single isolated sideband, as shown in Fig. 2. The sideband can be scanned through the spectral feature by tuning ω_c or ω_m. In either case, the losses and phase shifts experienced by the carrier and lower sideband remain essentially constant. Thus $\delta_{-1}=\delta_0=\bar{\delta}$ and $\phi_{-1}=\phi_0=\bar{\phi}$, where $\bar{\delta}$ and $\bar{\phi}$ are the constant background loss and phase shift, respectively. If the quantities $\Delta\delta$ and $\Delta\phi$ are defined to express the deviations from the background values caused by the spectral feature, then

$$I_3(t)=\frac{cE_0^2}{8\pi}e^{-2\bar{\delta}}(1-\Delta\delta M\cos\omega_m t+\Delta\phi M\sin\omega_m t). \quad (4)$$

The $\cos\omega_m t$ and $\sin\omega_m t$ components of the beat signal are thus, respectively, proportional to the absorption and dispersion induced by the spectral feature.

The rf beat signal arises from a heterodyning of the FM sidebands and thus the signal strength is proportional to the geometrical mean of the intensities of one sideband and of the carrier. Thus the signal strength is proportional to $E_0^2 M$, while the intensity of the probing sideband is $I=cE_0^2M^2/8\pi$. Because of the different M dependence, arbirarily large signal strengths can be achieved for arbitrarily low sideband intensities by properly adjusting the values of E_0 and M. The perturbing effects of the probing sideband on the spectral feature can thus be minimized. The null signal that occurs when the FM spectrum is not distorted, can be thought of as arising from a perfect cancellation of the rf signal due to the upper sideband beating against the carrier with the rf signal arising from the lower sideband beating against the carrier. The high sensitivity to the phase or amplitude changes experienced by one of the sidebands results from the disturbance of this perfect cancellation.

For many applications, the spectral feature of interest has a Lorentzian or near Lorentzian lineshape. The lineshapes of the corresponding FM spectroscopy signals depend critically on the ratio of sideband spacing to the Lorentzian linewidth. It is convenient to define the spectral dependence of the dimensionless attenuation δ and phase shift ϕ by the relations

$$\delta(\omega)=\delta_{\text{peak}}\left(\frac{1}{R^2(\omega)+1}\right), \quad (5)$$

$$\phi(\omega)=\delta_{\text{peak}}\left(\frac{R(\omega)}{R^2(\omega)+1}\right), \quad (6)$$

where δ_{peak} is the peak attenuation at line center, Ω is the line center frequency, $\Delta\Omega$ is the full width at half maximum, and R is a normalized frequency scale defined by

$$R(\omega)=\frac{\omega-\Omega}{(\Delta\Omega/2)}. \quad (7)$$

Thus, $\delta(\Omega)=\delta_{\text{peak}}$ and $\phi(\Omega)=0$. Equations (5–7) define $\delta_j=\delta(\omega_j)$ and $\phi_j=\phi(\omega_j)$ for each spectral component of the FM optical spectrum. Again, the subscript $j=0, \pm 1$ denotes the values at frequencies ω_c and $\omega_c\pm\omega_m$, respectively. Substitution of these results in (3) gives a complete specification of the FM signal lineshape obtained when ω_c or ω_m is scanned.

It is often experimentally convenient to scan the sidebands through the spectral feature by tuning the laser carrier frequency ω_c with the rf modulation frequency ω_m held constant. Figures 3 and 4 show the various possible heterodyne beat signals as function of the normalized parameter $R_0=R(\omega_c)$ which denotes

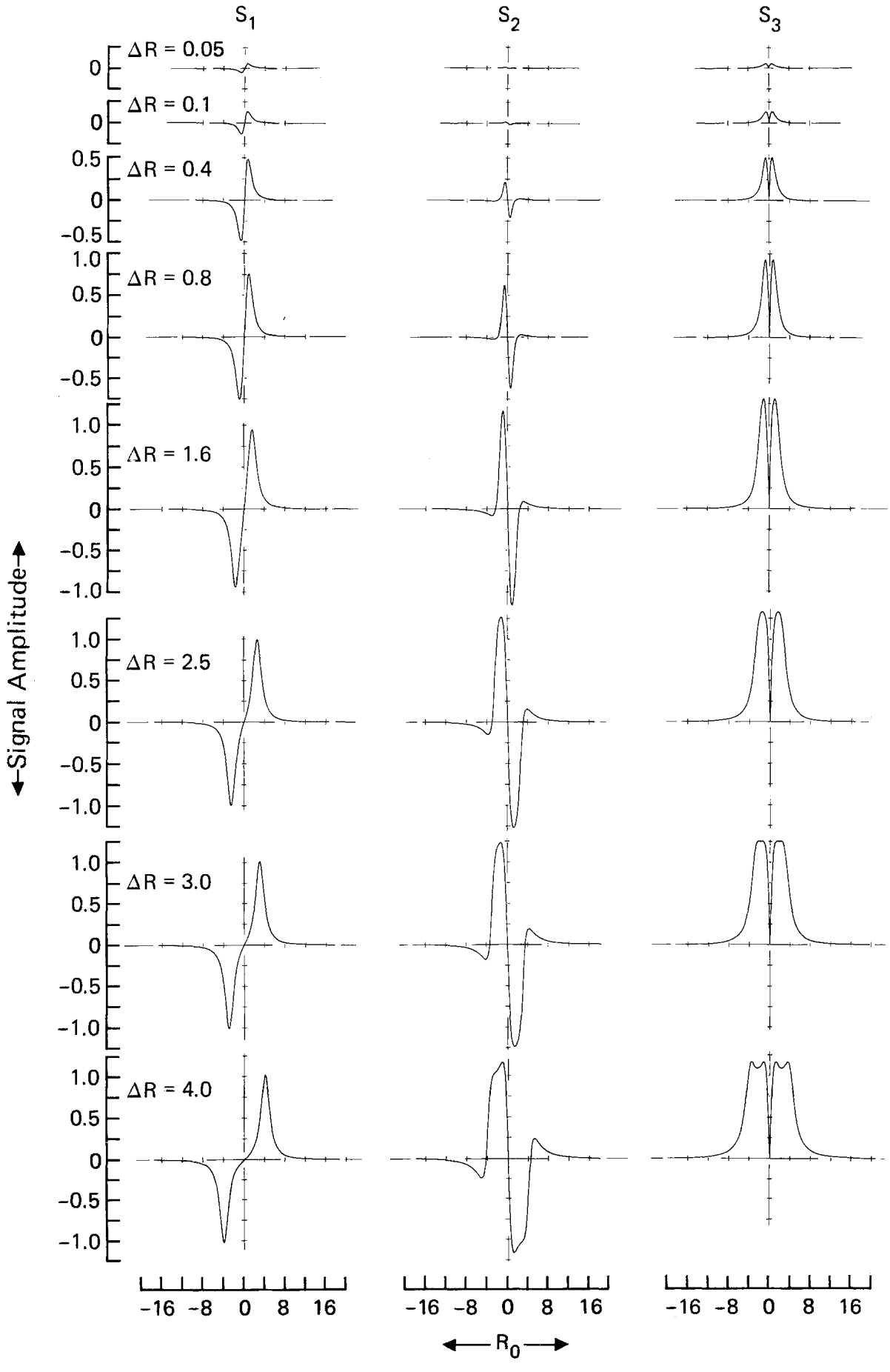

Fig. 3. Heterodyne beat signals S_1, S_2, and S_3, vs. R_0 for $0.05 \leqq \Delta R \leqq 4.0$

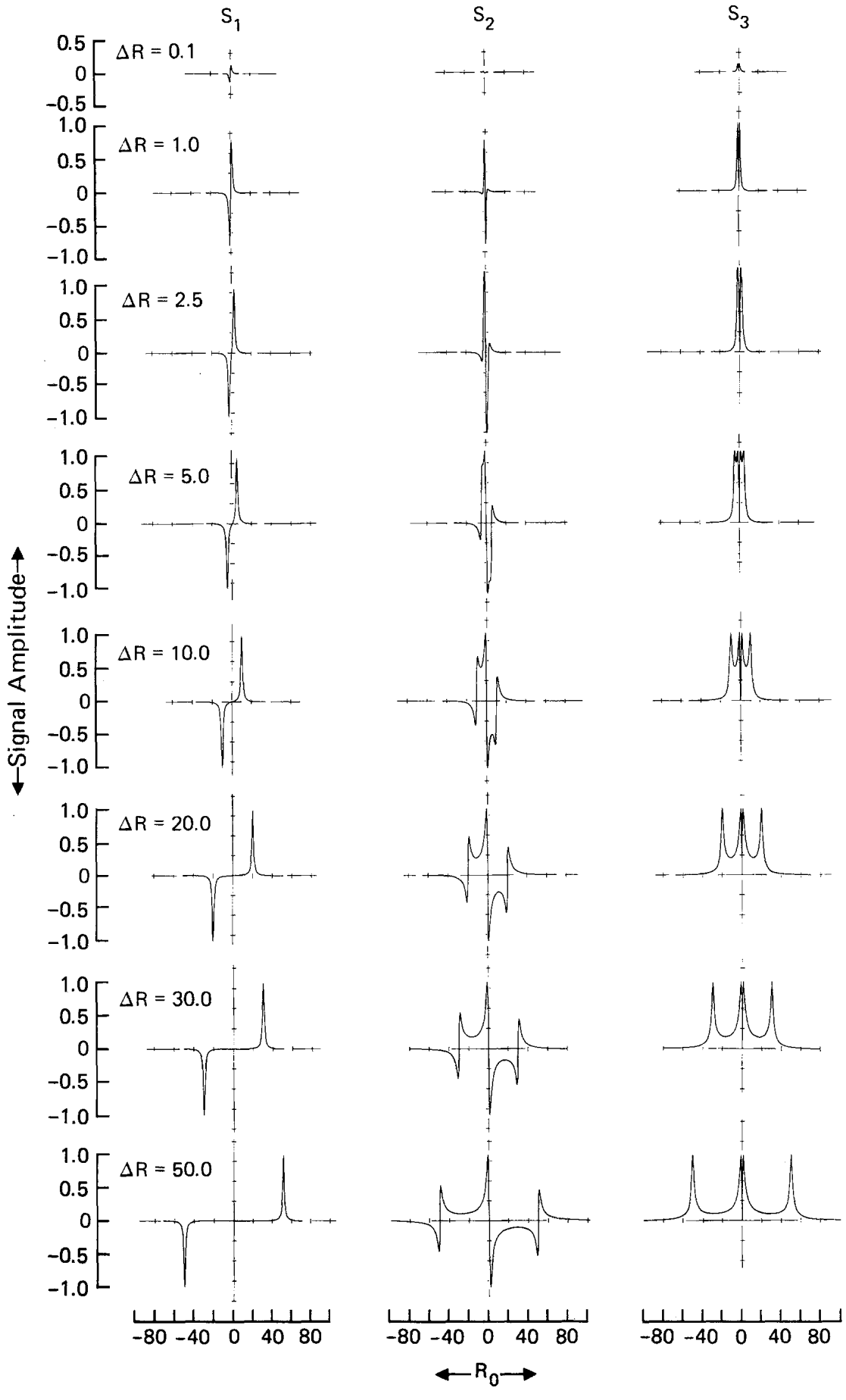

Fig. 4. Heterodyne beat signals S_1, S_2, and S_3 vs. R_0 for $0.1 \leqq \Delta R \leqq 50.0$

the relative position of the carrier frequency with respect to the resonance. Here each curve corresponds to R_0 being smoothly tuned through the vicinity of the spectral feature with a constant sideband spacing described in terms of the parameter $\Delta R = \omega_m/(\Delta\Omega/2)$ and with δ_{peak} equal to unity. When $R_0 = -\Delta R$, the $\omega_c + \omega_m$ sideband is resonant with the spectral feature; when $R_0 = 0$, the ω_c carrier is resonant; and when $R_0 = \Delta R$, the $\omega_c - \omega_m$ sideband is resonant.

The column denoted S_1 shows the amplitude of the absorption ($\cos\omega_m t$) signal, the column denoted S_2 shows the amplitude of the dispersion ($\sin\omega_m t$) signal, and column $S_3 = \sqrt{S_1^2 + S_2^2}$ shows the modulus of the total beat signal. S_1 and S_2 corresponds to *dc* signals which could be directly observed using the exact set-up shown in Fig. 1, provided that the phase adjuster is set properly. Intermediate settings of the phase adjuster produce mixed lineshapes. S_3 corresponds to the signal which could be directly observed using a phase insensitive detector such as a spectrum analyzer to process the photodiode signal.

The evolution from the wavelength modulation to the FM spectroscopy limits can clearly be seen. For $\Delta R \leqq 0.1$, S_1 is very close to the derivative of the absorption and S_2 is very weak. For $0.1 \leqq \Delta R \leqq 1.6$, S_1 reaches its full strength and becomes a somewhat distorted derivative lineshape, while S_2 grows rapidly in strength. It is interesting to note that, aside from polarity, in this region the shape of S_2 resembles that of S_1. For $3 \leqq \Delta R \leqq 5$, S_1 begins to show separate resonances as the upper and lower frequency sidebands probe the spectral feature. However, S_2 and S_3 do not yet show resolved resonances, although for $\Delta R \simeq 4$, the curves show a pronounced "flattening" at the extrema. For $\Delta R > 5$, the S_1 resonances become very close to the Lorentzian absorption lineshape. S_2 begins to show resolved dispersion shaped resonances as the upper sideband, carrier, and then the lower sideband probe the feature. S_3 also begins to show resonances at these locations. Since both the S_2 and S_3 resonances fall off linearly with detuning, substantial overlap occurs even for ΔR as large as 50. The S_3 lineshape always dips sharply to exact zero when $R_0 = 0$ corresponding to the carrier tuned to exact line center. In fact, for all values of ΔR, $S_1 = S_2 = S_3 = 0$ when $R_0 = 0$. This property of FM spectroscopy is useful in frequency locking applications.

Signal-to-Noise Analysis

For simplicity, we consider the case where a purely absorptive spectral feature is probed with a single isolated sideband and no background absorption is present. Then, from (4), with $\Delta\phi = \bar{\delta} = 0$, the slowly varying envelope $P_3(t)$ of the optical power incident on a photoconductor of area A is given by

$$P_3(t) = P_0(1 - \Delta\delta M \cos\omega_m t), \tag{8}$$

where $P_3(t) = AI_3(t)$ and $P_0 = AcE_0^2/8\pi$ is the total laser power. The current $i(t)$ generated by a photodetector of quantum efficiency η and gain g is $i(t) = \bar{i} + i_s(t)$ where the *dc* photocurrent is given by

$$\bar{i} = ge\eta \frac{P_0}{\hbar\omega_m} \tag{9}$$

and the beat signal photocurrent is

$$i_s(t) = -ge\eta \frac{P_0}{\hbar\omega_c} \Delta\delta M \cos\omega_m t. \tag{10}$$

Thus the rms power of the beat signal is given by

$$\overline{i_s^2(t)} = \frac{1}{2} g^2 e^2 \eta^2 \left(\frac{P_0}{\hbar\omega_c}\right)^2 \Delta\delta^2 M^2. \tag{11}$$

Since $1/f$ amplitude noise is insignificant at rf frequencies for single-mode lasers, the dominant sources of noise are thermal noise and shot noise generated at the photodetector. The rms noise power is given by

$$\bar{i}_N^2 = \bar{i}_{SN}^2 + \bar{i}_{TH}^2, \tag{12}$$

where the shot noise power is

$$\bar{i}_{SN}^2 = 2eg\bar{i}\Delta f = 2g^2 e^2 \eta \left(\frac{P_0}{\hbar\omega_c}\right) \Delta f, \tag{13}$$

and the thermal noise power is

$$\bar{i}_{TH}^2 = \left(\frac{4kT}{R}\right) \Delta f. \tag{14}$$

Here Δf is the bandwidth of the detection electronics, k is Boltzman's constant, T is the temperature in K, and R is the input impedance of the detection electronics. The ratio of signal-to-noise (S/N) is

$$\frac{S}{N} = \frac{\overline{i_s^2(t)}}{\bar{i}_N^2} = \frac{\frac{1}{2} g^2 e^2 \eta^2 \left(\frac{P_0}{\hbar\omega_c}\right)^2 \Delta\delta^2 M^2}{2g^2 e^2 \eta \left(\frac{P_0}{\hbar\omega_c}\right) \Delta f + \left(\frac{4kT}{R}\right) \Delta f}. \tag{15}$$

From (15), it can be seen that it is always advantageous to increase the total laser power P_0, to increase the modulation index M, to have η near unity, and to work with narrow band detection electronics.

When $P_0 \geqq P_{0\min} = 2kT\hbar\omega_c/\eta g^2 e^2 R$, shot noise predominantes over thermal noise. For photomultipliers, typical values are $\hbar\omega_c = 3 \times 10^{-19}$ J, $\eta = 0.1$, $g = 10^5$, $R = 50\,\Omega$, and $T = 300$ K, yielding $P_{0\min} = 2 \times 10^{-12}$ W. For photodiodes, typical values for η and g are both 1, yielding $P_{0\min} = 2 \times 10^{-3}$ W. Under these shot noise

limited conditions,

$$\frac{S}{N}=\frac{\eta\left(\frac{P_0}{\hbar\omega_c}\right)\Delta\delta^2 M^2}{4\Delta f} \tag{16}$$

and the minimum absorption, $\Delta\delta_{\min}$, detectable with unity S/N in an integration time $\tau=1/\Delta f$ is

$$\Delta\delta_{\min}=2\left[\eta M^2\left(\frac{P_0}{\hbar\omega_c}\right)\tau\right]^{-1/2}. \tag{17}$$

The quantity $M^2(P_0/\hbar\omega_c)\tau$ is four times the total number of photons in a sideband arriving during interval τ. Assuming $\eta=1$, $P_0=5\times10^{-3}$ W, and $M=0.1$, a value of $\Delta\delta_{\min}=1.5\times10^{-7}$ should be detectable for $\tau=1$ s and $\Delta\delta_{\min}=0.005$ should be detectable for $\tau=10^{-9}$ s.

Actually achieving quantum noise limited detection sensitivity requires careful attention to experiment detail. Several additional effects can degrade the sensitivity, but correct experimental practice can reduce or eliminate their impact. In the following, we discuss a few of these effects on a phenomenological basis.

It is important that the rf oscillator producing the modulation frequency ω_m be as stable as possible. Fluctuations in the phase or frequency of the oscillator produce noise at the double balanced mixer when the propagation times between the oscillator and the mixer for the optical signal differs from that for the local oscillator. The mixer then multiplies an electrical signal produced by the oscillator at one time with that produced at a different time, and possibly with a different phase. The result is a noisy dc signal. One characteristic of this kind of noise is that its amplitude depends on the phase shift introduced by the phase adjuster shown in Fig. 1. There is always one phase where the noise is minimized. Another strategy for minimizing this oscillator instability noise is to add delay lines between the oscillator and the double balanced mixer until the propagation paths for signal and local oscillators are equal.

A second noise source results from the fact that available optical phase modulators do not produce the pure FM spectrum illustrated by (1). Rather, there is always a small component at ω_m that results from a small imbalance in the amplitudes of the sidebands or a relative shift in phase which prevents the beat frequency from vanishing exactly. This residual AM can be detected by the photodiode and introduces a nonzero baseline. More seriously, the residual AM amplitude is modulated by the power fluctuations of the laser, and thus the level of the baseline fluctuates and introduces noise in the dc output signal. This noise can be minimized by carefully aligning the input and output polarizations of the modulator to balance the sidebands and by adjusting the relative phase of the local oscillator and signal to minimize the offset due to residual AM. Acceptable FM signals can then be obtained even with a relatively noisy laser and an unbalanced phase modulator.

Finally, at the low signal levels described by (17) with a 1-s integration time τ, variations in the rf pickup due to movements in the laboratory can introduce drifts and noise. It is important to shield the detection apparatus from electromagnetic interference radiated by the relatively strong amplifier necessary to drive the modulator. With due care, quantum noise limited sensitivity to modulated absorptions can readily be approached with FM spectroscopy [25, 38].

Conclusions

Sensitive and rapid detection of narrow spectral features can be accomplished using FM spectroscopy. Since the heterodyne beat signals occur at rf frequencies where single-mode dye lasers are relatively noise free, shot noise limited detection is possible. The entire spectral feature can be scanned by tuning either the laser carrier frequency or the rf modulation frequency. The detailed lineshape of the FM spectroscopy signal depends on the phase of the rf detection electronics and on the ratio of the rf modulation frequency to the with of the spectral feature.

Acknowledgement. The authors wish to thank L. Pawlowicz and J.R. DeLany for help in preparing the figures.

References

1. G.C. Bjorklund: IBM Invention Disclosure SA 8790135 (March 1979)
   G.C. Bjorklund: Opt. Lett. **5**, 15 (1980)
   G.C. Bjorklund: U.S. Patent 4,297,035 (November 1981)
2. This technique was independently suggested by R.W.P. Drever as a means for servo-locking a tunable laser to a high finesse optical cavity. It was first experimentally implemented for this purpose by R.W.P. Drever, J.L. Hall, F.V. Kowalski, J. Hough, G.M. Ford, A.J. Munley (September 1979) and then by M. Prentiss, B. Peuse, G. Sanders, S. Ezekiel: Research Laboratory of Electronics, Progress Report No. 123 (January 1981) (Massachusetts Institute of Technology, Cambridge, MA)
3. R.V. Pound: Rev. Sci. Instrum. **17**, 490 (1946)
4. B. Smaller: Phys. Rev. **83**, 812 (1951)
5. J.V. Acrivos: J. Chem. Phys. **36**, 1097 (1962)
6. V.J. Corcoran, R.E. Cupp, J.J. Gallagher, W.T. Smith: Appl. Phys. Lett. **16**, 316 (1970)
7. A.T. Mattick, A. Sanchez, N.A. Kurnit, A. Javan: Appl. Phys. Lett. **23**, 675 (1973)
8. G. Magerl, E. Bonek, W.A. Kreiner: Chem. Phys. Lett. **52**, 473 (1977)
9. A. Szabo: Phys. Rev. B**11**, 4512 (1975)
10. L.E. Erickson: Phys. Rev. B**16**, 4731 (1977)

11. J.J. Snyder, R.K. Raj, D. Bloch, M. Ducloy: Opt. Lett. **5**, 163 (1980)
12. R.K. Raj, D. Bloch, J.J. Snyder, G. Camy, M. Ducloy: Phys. Rev. Lett. **44**, 1251 (1980)
13. D. Bloch, M. Ducloy, E. Giacobino: J. Phys. B **14**, L 819 (1981)
14. M. Ducloy, D. Bloch: J. Phys. (Paris) **43**, 57 (1982)
15. E.D. Hinkley, P.L. Kelley: Science **171**, 635 (1971)
16. C.L. Tang, J.M. Telle: J. Appl. Phys. **45**, 4503 (1974)
17. S.E. Harris, M.K. Oshman, B.J. McMurtry, E.O. Ammann: Appl. Phys. Lett. **7**, 185 (1975)
18. G.C. Bjorklund, M.D. Levenson: Phys. Rev. A **24**, 166 (1981) G.C. Bjorklund, W. Lenth, M.D. Levenson, C. Ortiz: SPIE **286**, 153 (1981)
19. J.L. Hall, L. Hollberg, T. Baer, H.G. Robinson: Appl. Phys. Lett. **39**, 680 (1981) and *Laser Spectroscopy V*, ed. by A.R.W. McKellar, T. Oka, B.P. Stoicheff (Springer, Berlin, Heidelberg, New York 1981) p. 15
20. W. Lenth, C. Ortiz, G.C. Bjorklund: Opt. Lett. **6**, 351 (1981)
21. G.C. Bjorklund, W. Lenth, M.D. Levenson, C. Ortiz: In *Laser Spectroscopy V*, ed. by A.R.W. McKellar, T. Oka, B.P. Stoicheff (Springer, Berlin, Heidelberg, New York 1981) p. 389
22. W. Lenth, G.C. Bjorklund, C. Ortiz: In *Proc. of the Lasers '81 Conference*, New Orleans, Lousiana (in press)
23. W. Zapka, P. Pokrowsky, F.M. Schellenberg, G.C. Bjorklund: Opt. Commun. **44**, 117 (1982)
24. W. Zapka, M.D. Levenson, F.M. Schellenberg, A.C. Tam, G.C. Bjorklund: Opt. Lett. **8**, 27 (1983)
25. M.D. Levenson, W.E. Moerner, D.E. Horne: Opt. Lett. **8**, 108 (1983)
26. P. Pokrowsky, E.A. Whittaker, G.C. Bjorklund: Opt. Commun. **45**, 196 (1983)
27. E.A. Whittaker, P. Pokrowsky, W. Zapka, K. Roche, G.C. Bjorklund: J. Quant. Spectrosc. Radiat. Transf. **30** (1983, in press)
28. G.S. Agarwal: Phys. Rev. A **23**, 1375 (1981)
29. A. Schenzle, R.G. DeVoe, R.G. Brewer: Phys. Rev. A **25**, 2606 (1982)
30. J.H. Shirley: Opt. Lett. **7**, 537 (1982)
31. E.A. Whittaker, G.C. Bjorklund: Paper FG1, Conference on Lasers and Electro-Optics, May 17–20, 1983, Baltimore, Maryland
32. G.A. Sanders, M.G. Prentiss, S. Ezekiel: Opt. Lett. **6**, 569 (1981)
33. R.G. DeVoe, R.G. Brewer: Phys. Rev. Lett. **50**, 1269 (1983) R.G. DeVoe, R.G. Brewer: Phys. Rev. A **26**, 705 (1982)
34. R.W.P. Drever, J.L. Hall, F.V. Kowalski, J. Hough, G.M. Ford, A.J. Munley, H. Ward: Appl. Phys. B **31**, 97 (1983)
35. W. Lenth et al.: To be published
36. T.F. Gallagher, R. Kachru, F. Gounand, G.C. Bjorklund, W. Lenth: Opt. Lett. **7**, 28 (1982)
37. N.H. Tran, R. Kachru, T.F. Gallagher, J.P. Watjen, G.C. Bjorklund: Opt. Lett. **8**, 157 (1983)
38. E.A. Whittaker, H.R. Wendt, H. Hunziker, G.C. Bjorklund: To be published